Acknowledgements

Amino acid display was performed using the program ASAD developed by Keith Satterly, WEHI, and is available by anonymous ftp from: ftp.wehi.edu.au/pub/biology/ASAD. This work was supported by the Anti-Cancer Council of Victoria.

References

1 Vaux, D. L., Weissman, I. L. and Kim, S. K. (1992) *Science* 258, 1955–1957
2 Hengartner, M. O. and Horvitz, H. R. (1994) *Cell* 76, 665–676
3 Miura, M., Zhu, H., Rotello, R., Hartweig, E. A. and Yuan, J. (1993) *Cell* 75, 653–660
4 Crook, N. E., Clem, R. J. and Miller, L. K. (1993) *J. Virol.* 67, 2168–2174
5 Birnbaum, M. J., Clem, R. J. and Miller, L. K. (1994) *J. Virol.* 68, 2521–2528
6 Vucic, D., Kaiser, W. J., Harvey, A. J. and Miller, L. K. (1997) *Proc. Natl. Acad. Sci. U. S. A.* 94, 10183–10188
7 Hay, B. A., Wassarman, D. A. and Rubin, G. M. (1995) *Cell* 83, 1253–1262
8 Liston, P. *et al.* (1996) *Nature* 379, 349–353
9 Uren, A. G., Pakusch, M., Hawkins, C. J., Puls, K. L. and Vaux, D. L. (1996) *Proc. Natl. Acad. Sci. U. S. A.* 93, 4974–4978
10 Hawkins, C. J., Uren, A. G., Hacker, G., Medcalf, R. L. and Vaux, D. L. (1996) *Proc. Natl. Acad. Sci. U. S. A.* 93, 13786–13790
11 Duckett, C. S. *et al.* (1996) *EMBO J.* 15, 2685–2694
12 Ambrosini, G., Adida, C. and Altieri, D. C. (1997) *Nat. Med.* 3, 917–921
13 Clem, R. J. and Miller, L. K. (1993) *J. Virol.* 67, 3730–3738
14 Roy, N. *et al.* (1995) *Cell* 80, 167–178
15 Rothe, M., Pan, M. G., Henzel, W. J., Ayres, T. M. and Goeddel, D. V. (1995) *Cell* 83, 1243–1252
16 Deveraux, Q. L., Takahashi, R., Salvesen, G. S. and Reed, J. C. (1997) *Nature* 388, 300–304
17 Roy, N., Deveraux, Q. L., Takahashi, R., Salvesen, G. S. and Reed, J. C. (1997) *EMBO J.* 16, 6914–6925
18 Harvey, A. J., Soliman, H., Kaiser, W. J. and Miller, L. K. (1997) *Cell Death Differ.* 4, 733–744
19 Pearson, W. R. and Lipman, D. J. (1988) *Proc. Natl. Acad. Sci. U. S. A.* 85, 2444–2448
20 Cockwell, K. Y. and Giles, I. G. (1989) *Comput. Appl. Biosci.* 5, 227–232
21 Hofmann, K., Bucher, P. and Tschopp, J. (1997) *Trends Biochem. Sci.* 22, 155–156
22 Thompson, J. D., Higgins, D. G. and Gibson, T. J. (1994) *Nucleic Acids Res.* 22, 4673–4680

ANTHONY G. UREN, ELIZABETH J. COULSON AND DAVID L. VAUX

The Walter and Eliza Hall Institute of Medical Research, Post Office Royal Melbourne Hospital, Victoria 3050, Australia.
Email: vaux@wehi.edu.au

The danger of metabolic pathways with turbo design

Bas Teusink, Michael C. Walsh, Karel van Dam and Hans V. Westerhoff

Many catabolic pathways begin with an ATP-requiring activation step, after which further metabolism yields a surplus of ATP. Such a 'turbo' principle is useful but also contains an inherent risk. This is illustrated by a detailed kinetic analysis of a paradoxical *Saccharomyces cerevisiae* mutant; the mutant fails to grow on glucose because of overactive initial enzymes of glycolysis, but is defective only in an enzyme (trehalose 6-phosphate synthase) that appears to have little relevance to glycolysis. The ubiquity of pathways that possess an initial activation step, suggests that there might be many more genes that, when deleted, cause rather paradoxical regulation phenotypes (i.e. growth defects caused by enhanced utilization of growth substrate).

A STRATEGY FOLLOWED by many catabolic pathways is that of first 'activating' a substrate in a reaction that requires ATP. In glycolysis, ATP is invested at the hexokinase (HK) and phosphofructokinase (PFK) steps; in (α and β) fatty acid oxidation, ATP is invested when fatty-acyl-coenzyme A is formed; and in active transport systems, ATP is invested in order to get substrates into cells. The investment of ATP is subsequently recouped, because a surplus of ATP is generated further down the pathway (Fig. 1a). One feasible reason for these activation steps is that they help to make these and the subsequent steps in the pathway thermodynamically downhill[1]. The principle of the turbo engine is similar: exhaust gases are fed back to enhance the fuel-input step (Fig. 1b). It has been suggested that a 'turbo design' of catabolic pathways is the result of evolutionary optimization with respect to flux – at least for glycolysis[2,3].

Biologically, it might be expected that the turbo principle would be most useful when there is a continuous supply of substrate – as is the case in multicellular organisms that maintain internal homeostasis. In many other (micro-) organisms, however, where the availability of substrate can be highly variable, such a turbo design could be a mixed blessing. In this paper we suggest that the striking phenomenon of substrate-accelerated death, which has been observed both in prokaryotes and in eukaryotes such as *S. cerevisiae*, could be the consequence of such a turbo design. Substrate-accelerated death has been observed when cells are subjected to an excess of a substrate that previously limited growth in continuous culture[4,5]. In (wild-type) yeast, substrate-accelerated death has been observed for maltose[6], but not for glucose (see Ref. 7, for example). This suggests that there are specific regulatory mechanisms that prevent a lethal effect of the sudden availability of glucose.

Genetic studies in *S. cerevisiae* have generated mutants that appear highly paradoxical [e.g. *fdp1* (Ref. 8), *cif1* (Ref. 9), *byp1* (Refs 10, 11)]. These mutants are unable to grow on high concentrations of glucose, even though the first steps in glycolysis seem to be activated rather than impaired. The mutants therefore appear to be defective in a regulatory mechanism that should prevent

B. Teusink, M. C. Walsh, K. van Dam and **H. V. Westerhoff** are at the E. C. Slater Institute, BioCentrum Amsterdam, University of Amsterdam, Plantage Muidergracht 12, NL-1018 TV Amsterdam, The Netherlands; and **H. V. Westerhoff** is also at IMBS, BioCentrum Amsterdam, Dept of Microbial Physiology, Faculty of Biology, Vrije Universiteit, De Boelelaan 1087, NL-1081 HV Amsterdam, The Netherlands.
Email: hw@bio.vu.nl

 0968–0004/98/$19.00 PII: S0968-0004(98)01205-5

glucose-accelerated death in yeast. Using a mathematical model of yeast glycolysis, we present an explanation for the phenotype of these particular *S. cerevisiae* mutants. Unexpectedly, the turbo design of yeast glycolysis appears to be central to the metabolic problems experienced by these mutants. Our analysis shows that metabolic pathways with turbo design require special types of regulation in environments that have rapidly changing substrate availability.

The phenotype of the *tps1-Δ* mutant

The *fdp1*, *cif1* and *byp1* mutants are unable to grow on glucose. It was surprising to find that the mutations are allelic[12] and that the primary lesion is in the *TPS1* gene, which encodes trehalose 6-phosphate (Tre 6-*P*) synthase[13–15]. Up until then, trehalose synthesis was considered to be a branch of glycolysis with no function other than in the formation of storage carbohydrates and the acquisition of stress tolerance[16]. Very little trehalose is made during exponential growth on glucose[17]; consequently, it seems puzzling that trehalose metabolism is needed for growth on glucose.

A *TPS1* disruptant accumulates hexose phosphates, but consumes ATP and inorganic phosphate rapidly[8,9,12,18–20]. No steady state is attained and the accumulation of hexose phosphates continues until all phosphate has been incorporated into sugar phosphates. The first steps of glycolysis appear to be too fast for the rest of the yeast's metabolism to cope with[13].

It is now clear that a metabolic function of Tps1p is to inhibit (one of) the first steps of glycolysis and thereby restrict the flux of glucose into glycolysis[13]. In *tps1-Δ* mutants, growth on glucose can be restored by reducing HK[19] or glucose transporter activity[21]. The finding that Tre 6-*P*, the metabolic product of Tps1p, inhibits HK *in vitro*, suggests a direct mechanism for HK inhibition in wild-type cells[22]; however, the possibility that Tps1p interacts directly with a glucose transporter and HK cannot be excluded[13,20,23]. In this paper, we shall not discuss the exact molecular mechanism of inhibition, but rather address the question of why and when such a 'guard at the gate of glycolysis' is required[13].

Simulation of glycolysis without feedback inhibition of hexokinase (HK)

We have examined the behaviour of a core model of yeast glycolysis that lacks any special regulation of the first ATP-consuming step. Focusing on the essentials, this model consists of only four steps: the HK reaction, the PFK reaction, the 'lower part' of glycolysis, and a general ATPase to remove the excess ATP produced by glycolysis (see Fig. 2, and Box 1 for details of stoichiometry and enzyme kinetics). Figure 3a,b shows a time course for this model at high glucose concentrations (i.e. high relative to the affinity of the HK block for glucose). Without feedback inhibition of HK, hexose monophosphate and fructose 1,6-bisphosphate (Fru 1,6-P_2) accumulated, and the ATP concentration barely recovered from an initial drop to below 0.3 mM (Fig. 3a). Although hexose phosphate levels did not reach a steady state, the rates of the reactions became constant (Fig. 3b), as did the ATP level.

The concentration of ATP remains constant whenever the rate of ATP consumption ($v_{consumption}$) is equal to the rate of ATP production ($v_{production}$). In the model, the following relationship should then hold:

$$v_{consumption} (= v_{HK} + v_{PFK} + v_{ATPase}) \quad (1)$$
$$= v_{production} (= 4v_{lower})$$

The data in Fig. 3a confirm that this is the case for our core model: after about ten minutes, the rates of the reactions fulfilled the above relationship and, therefore, the level of ATP became constant.

The system will only reach a true steady state when two criteria are satisfied: (1) the rates of the HK reaction, the PFK reaction and the lower part of glycolysis are equal; (2) the rate of the ATPase reaction is twice that of the other steps. In the steady state, the following relationship will therefore apply:

$$v_{HK} = v_{PFK} = v_{lower} = 2v_{ATPase} \quad (2)$$

This second steady-state condition was *not* met in the simulation of unguarded glycolysis (i.e. the rate of the lower part of glycolysis did not become equal to those of the HK and PFK modules). Rather, the kinase fluxes greatly exceeded the flux through lower glycolysis ($v_{HK} > v_{PFK} > v_{lower}$; see Fig. 3b), causing the accumulation of both hexose monophosphate (because $v_{HK} > v_{PFK}$) and Fru 1,6-P_2 (because $v_{PFK} > v_{lower}$; see

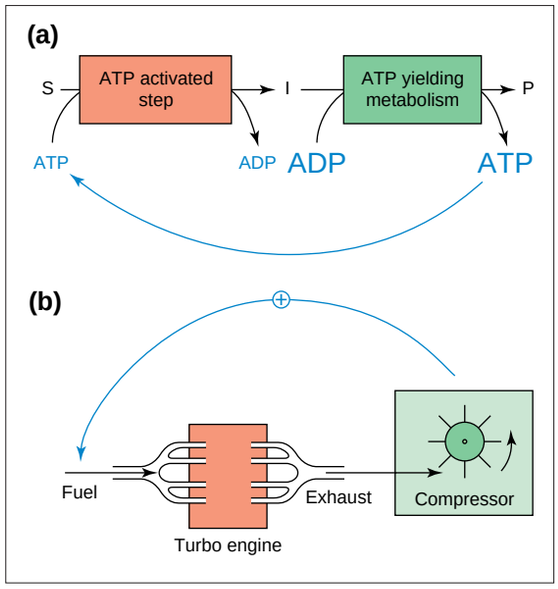

Figure 1
Comparison of an activated catabolic pathway with a turbo engine. **(a)** General scheme for a catabolic pathway in which the first step involves coupling of ATP hydrolysis to activation of a substrate (S). Downstream, the conversion of an intermediate (I) to a product (P) generates a surplus of ATP. **(b)** Schematic representation of a turbo engine, in which exhaust gases are used to increase the influx of fuel.

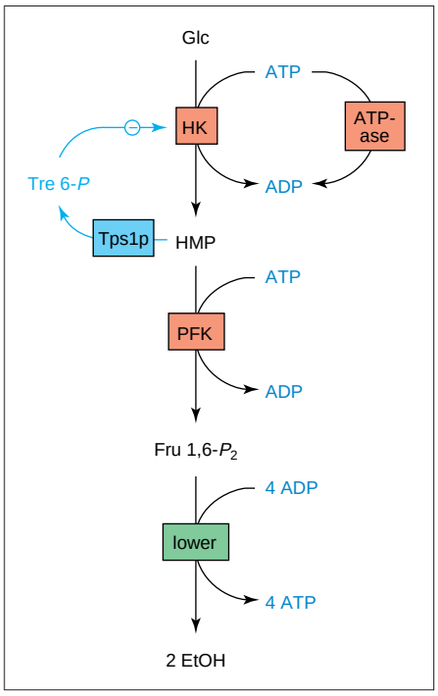

Figure 2
Schematic representation of the core model of glycolysis. See Box 1 for kinetic details of each step. In this model the lower part (downstream reactions) of glycolysis is represented by a single step. Glc, glucose; HMP, hexose monophosphate; Fru 1,6-P_2, fructose 1,6-bisphosphate; Tre 6-*P*, trehalose 6-phosphate; EtOH, ethanol; HK, hexokinase; PFK, phosphofructokinase; Tps1p, Tre 6-*P* synthase; lower, lower part of glycolysis.

Box 1. Description of the kinetic model

We have constructed a core model of glycolysis, consisting of hexokinase (HK) , phosphofructokinase (PFK), the lower part of glycolysis and a general ATPase, which consumes the ATP produced (Fig. 2). The independent metabolites in this model are ATP, hexose monophosphate (HMP; i.e. glucose 6-phosphate and fructose 6-phosphate) and fructose 1,6-bisphosphate (Fru 1,6-P_2). The model therefore comprises a set of three ordinary differential equations (see Fig. 2):

$$\frac{d[HMP]}{dt} = \nu_{HK} - \nu_{PFK} \qquad \frac{d[Fru\ 1,6\text{-}P_2]}{dt} = \nu_{PFK} - \nu_{lower} \qquad \frac{d[ATP]}{dt} = 4\nu_{lower} - \nu_{HK} - \nu_{PFK} - \nu_{ATPase}$$

Square brackets indicate the concentration of the metabolite; ν represents the rate of each enzyme-catalysed reaction. HK represents both the transport step and the HK reaction; it exhibits irreversible Michaelis–Menten kinetics with two substrates, glucose (Glc) and ATP:

$$\nu_{HK} = V_{HK}\frac{\frac{[Glc]}{K_{Glc}}\frac{[ATP]}{K_{ATP}}}{\left(1+\frac{[Glc]}{K_{Glc}}\left[+\frac{[Tre\ 6\text{-}P]}{K_{i,Tre\ 6\text{-}P}}\right]\right)\left(1+\frac{[ATP]}{K_{ATP}}\right)}$$

The term in square brackets was introduced only for the wild-type model, which exhibits trehalose 6-phosphate- (Tre 6-*P*) dependent feedback inhibition of the HK module (see below). The parameter values were as follows: V_{HK} = 68 mM min^{-1}; K_{ATP} = 0.15 mM; K_{Glc} = 1 mM; $K_{i,Tre\ 6\text{-}P}$ = 4.422 mM.

The kinetics of this module[33] are proposed to be dominated by HK (i.e. it is assumed that the glucose transporter does not exert a significant control on the flux through this module at the high glucose concentrations employed[34,35]). The HK is taken to be insensitive to its products (product inhibition by glucose-6-phosphate is very poor[36]).

Complete irreversibility and product insensitivity are simplifications that allow a rigorous analysis in terms of rate characteristics of the participating enzymes to be made (see Box 2). Including reversibility and weak product sensitivity in the model of unguarded glycolysis leads to a high, constant HMP level at which mass action and the weak inhibition become significant (B. Teusink, M. C. Walsh, K. van Dam and H. V. Westerhoff, unpublished; see Fig. 3a). This would not, however, alter the essence of the metabolic problem: accumulation of hexose phosphates at constant ATP levels. For the sake of analytical power, we have not considered these kinetic details in our core model.

Although the precise molecular mechanism of action of Tps1p is unclear, it is clear that Tps1p negatively affects the activity of the HK module – either through competitive inhibition of HK[22] or through the formation of a complex involving both the transporter and HK[13]. Here, we have used the competitive inhibition model because the alternative is difficult to describe in terms of a rate equation. Glucose 6-phosphate is a substrate of Tps1p and fructose 6-phosphate is an activator of Tps1p[15,37]. Rather than introducing a new variable into the model, we have used a simple quadratic relationship between the Tre 6-*P* concentration and that of the HMP concentration: [Tre 6-*P*]=[HMP]^2.

PFK is modelled as a two-substrate Monod–Wyman–Changeux enzyme[38], using the rate equation from Ref. 39 (also used in Ref. 40) with HMP and ATP as PFK substrates. A modification describing ATP inhibition, rather than AMP activation, has been incorporated because AMP is not considered in the core model. Other regulatory interactions of PFK have also been omitted for the sake of simplicity. The rate equation for PFK follows:

$$\nu_{PFK} = V_{PFK}\frac{g_R\lambda_1\lambda_2 R}{R^2 + LT^2}$$

The following expressions are defined:

$$\lambda_1 = [HMP]/K_{R,HMP}$$

$$\lambda_2 = [ATP]/K_{R,ATP}$$

$$\lambda_3 = [ATP]/K_{i,ATP}$$

$$R = 1 + \lambda_1 + \lambda_2 + g_R\lambda_1\lambda_2$$

$$T = 1 + c_1\lambda_1 + c_2\lambda_2 + g_T c_1\lambda_1 c_2\lambda_2$$

$$L = L_0\left(\frac{1 + c_i\lambda_3}{1 + \lambda_3}\right)^2$$

The parameters for the above expressions had the values: $K_{R,HMP}$ = 1 mM; g_R = 10; c_1 = 0.0005; L_0 = 1000; $K_{R,ATP}$ = 0.06 mM; g_T = 1; c_2 = 1; $K_{i,ATP}$ = 10 mM; V_{PFK} = 30 mM min^{-1}; c_i = 10.

The lower part of glycolysis (from aldolase to alcohol dehydrogenase) is also grouped into one module in the core model. The expression of most enzymes in this module – especially pyruvate decarboxylase – is glucose induced[41,42], suggesting that adaptation (in this module) is required for the switch from gluconeogenesis to glycolysis. An important assumption in our model is that, at the moment of glucose addition, the capacity of the lower part of glycolysis is lower than that of HK and PFK. The lower part of glycolysis is therefore modelled in such a way that it follows Michaelis–Menten kinetics (with Fru 1,6-P_2 and ADP as substrates) and its V_{max} is set at a level lower than that of PFK and HK:

$$\nu_{lower} = V_{lower}\frac{\frac{[Fru\ 1,6\text{-}P_2]}{K_{Fru\ 1,6\text{-}P_2}}\frac{(5-[ATP])}{K_{ADP}}}{\left(1+\frac{[Fru\ 1,6\text{-}P_2]}{K_{Fru\ 1,6\text{-}P_2}}\right)\left(1+\frac{(5-[ATP])}{K_{ADP}}\right)}$$

The parameters for the above expression had the values: V_{lower} = 20 mM min^{-1}; $K_{Fru\ 1,6\text{-}P_2}$ = 1 mM; K_{ADP} = 0.1 mM. The ADP concentration was taken as a function of the ATP concentration: [ADP] + [ATP] = constant = 5 mM.

(continued)

Box 1. Description of the kinetic model (contd)

The general ATPase is also described by Michaelis–Menten kinetics, with ATP as the substrate. The ATP dependency of the general ATPase in our model is justified by the experimental results of Buttgereit *et al.*[43], who showed that the rates of ATP-consuming processes depend on the availability of ATP. Although the kinetics of such a general ATPase are necessarily oversimplified, the details do not affect the conclusions of this paper (B. Teusink, M. C. Walsh, K. van Dam and H. V. Westerhoff, unpublished). The rate equation for the ATPase module was as follows:

$$v_{ATPase} = V_{ATPase} \frac{[ATP]}{K_{ATP} + [ATP]}$$

The parameters for the above expression had the values: V_{ATPase} = 68 mM min^{-1}; K_{ATP} = 3 mM. The models were run on a personal computer, using the metabolic modelling software SCAMP[44].

Fig. 3a). These results – especially the accumulation of hexose phosphates at constant ATP concentration – are consistent with the phenotype observed when a yeast *tps1-Δ* mutant is given high amounts of glucose (see Refs 20, 21 for clear examples of this phenotype).

A guard at the gate of glycolysis helps

Figure 3c,d presents data obtained for a model in which 'guarded' glycolysis is simulated. The guard is modelled as an inhibition of the HK module by hexose monophosphate (see Box 1 for details). For *S. cerevisiae*, this regulation would involve Tps1p. The introduction of such feedback inhibition was effective in restoring a steady state at high glucose concentrations. The hexose monophosphate, Fru 1,6-P_2 and ATP concentrations reached constant levels, and the ATP level was considerably higher than that in the unguarded glycolysis model (Fig. 3a). The rates of the HK reaction, the PFK reaction and the lower part of glycolysis did become equal, and that of the ATPase became twice that rate. The model in which regulation of the HK module occurs was therefore able to reach a complete steady state at high glucose levels – as wild-type yeast cells do.

Deletion of the HK PII gene (which encodes one of the three glucose phosphorylating enzymes) can suppress the phenotype of the *tps1-Δ* mutant in *S. cerevisiae*[19], and reduced glucose transport can do the same in *Kluyveromyces lactis*[21]. In Fig. 3e,f, we show data from a model in which, rather than introducing feedback inhibition, the activity of the HK module has been reduced to about 20% of its wild-type level. A reduction in the activity of the HK module led to restoration of a complete steady state (i.e. both the concentration of ATP and that of hexose phosphate became constant) – as in the case of feedback inhibition. We therefore conclude that our calculations confirm that feedback regulation at the gate of glycolysis is necessary, if a complete and viable steady state is to be achieved at high glucose concentrations.

Why does glycolysis go awry?

What exactly goes wrong in unguarded glycolysis? In the absence of feedback inhibition from hexose monophosphate to the HK module, the rest of metabolism can only communicate with the HK module via the ATP concentration. A detailed analysis of the ATP-dependency of the model's four modules is carried out in Box 2. In summary, it shows that the levels of hexose phosphate are not at steady state, because of the absence of a regulatory feedback mechanism between the upper and lower parts of glycolysis – other than ATP. Owing to the turbo design of glycolysis, there are two requirements if a steady state is to be achieved: the ATP production and consumption should be equal (see Eqn 1), and the rates of reactions of the enzymes in glycolysis should be equal (and twice that of the ATPase reaction; see Eqn 2). The latter condition implies the former, but not vice versa. It is apparent that, in the absence of feedback regulation of HK (as in the case of the *tps1-Δ* mutant), the ATP concentration is tuned to satisfy the former condition. ATP – as sole feedback regulator in this case – is ineffective because it becomes trapped at a concentration that tunes ATP production to ATP consumption (see Box 2). Being trapped in this 'ATP-steady' state, it can no longer serve to tune hexose phosphate synthesis to hexose phosphate degradation, and so the second condition is not satisfied. Wild-type yeast cells have the required extra feedback mechanism in the form of Tps1p. The case of reduced HK activity (Fig. 3e,f) demonstrates that such a feedback mechanism is only required when the capacity of the first (ATP-driven) reaction exceeds that of the later ATP-producing reaction.

Why did yeast evolve feedback of the HK module by Tps1p and not by direct product inhibition of HK?

Tps1p inhibits the HK module, either directly or through Tre 6-*P*. We introduced inhibition by Tre 6-*P* into our core model, and a quadratic relationship between the concentration of hexose monophosphate and that of Tre 6-*P* was employed (see Box 1). An obvious question is whether the feedback by Tps1p (through Tre 6-*P*) might not also be achieved by direct product inhibition of HK (by hexose monophosphate) – a phenomenon that is common in many mammalian systems. One important difference between mammalian cells and yeast cells is the relatively constant glucose concentration encountered by the former as compared with that encountered by the latter. It might be that regulation by Tps1p has evolved specifically to cope with sudden and large variations in the extracellular glucose concentration. This possibility is investigated in Table I, where the behaviours of four versions of the core model were calculated at an extracellular glucose concentration 100 times lower than that used in Fig. 3. Because of the low glucose concentration, all models reached a steady state, irrespective of the presence of feedback inhibition on the HK module. The steady-state concentrations of ATP, hexose monophosphate and Fru 1,6-P_2, and the steady-state flux through the modules were calculated for unguarded glycolysis, glycolysis with reduced HK activity and glycolysis with either of two types of feedback on the HK module: indirect, through Tre 6-*P*; or direct, through hexose monophosphate.

The version of the core model representing the *tps1-Δ* mutant (unguarded glycolysis) showed a higher steady-state glycolytic flux and a higher steady-state ATP level compared with the other versions. In the version with reduced HK activity, the rate of ATP consumption was always higher than that of ATP production (owing to the activity of the ATPase), and the level of ATP rapidly decreased to zero; the fluxes were therefore zero as well. In the version in which Tre-6-*P*-mediated feedback inhibition of HK occurs, which ensured a steady state at high glucose concentrations (Fig. 3b,c), the flux and steady-state ATP concentration were about half those of the version of the model representing the *TPS1* deletant.

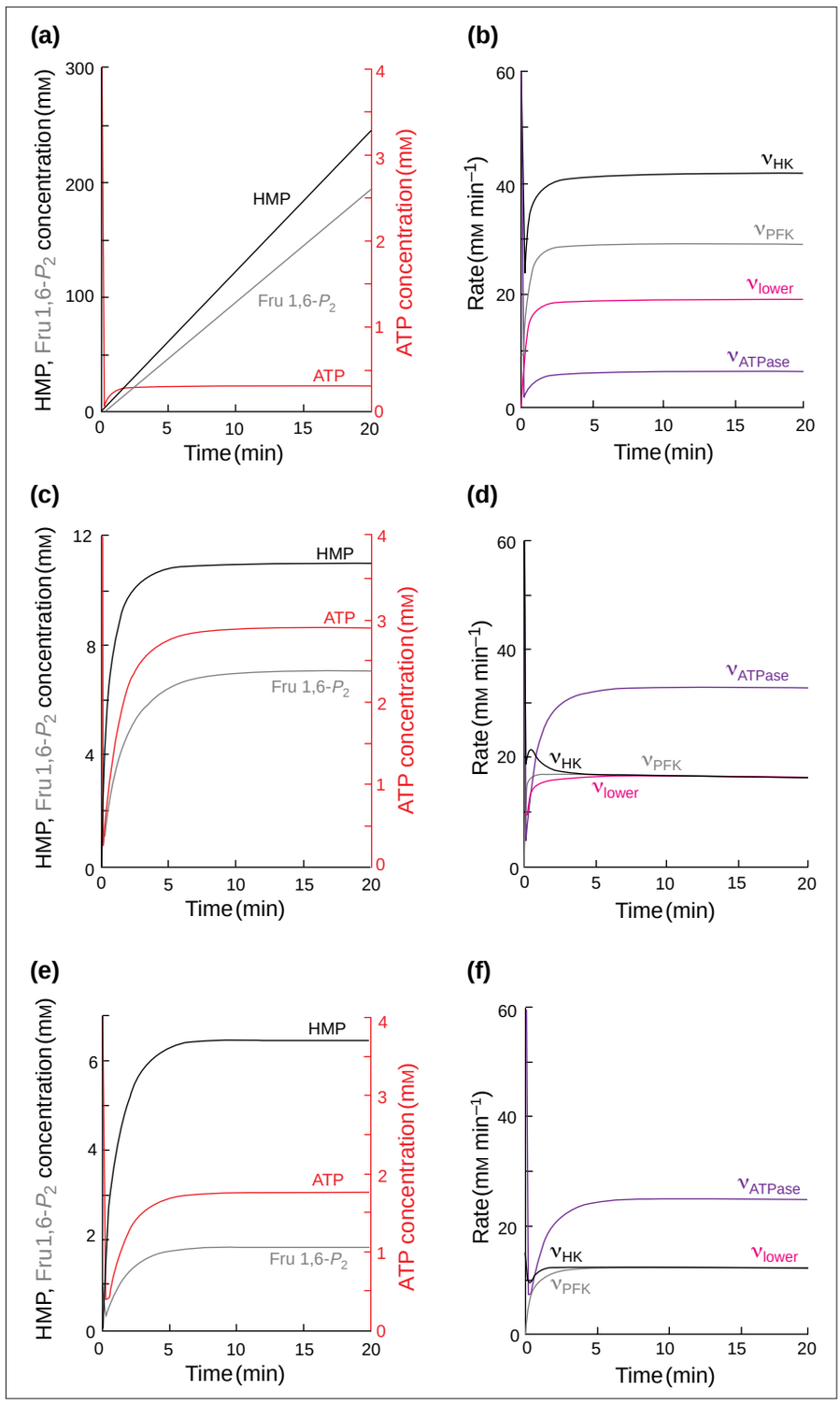

Figure 3

Simulations of time courses for the core model of glycolysis (Fig. 2) in three different cases. **(a,b)** Unguarded glycolysis. **(c,d)** Glycolysis with product inhibition of hexokinase (HK). **(e,f)** Unguarded glycolysis with reduced HK activity. In all cases, the initial concentrations of hexose monophosphate (HMP), fructose 1,6-bisphosphate (Fru 1,6-P_2) and ATP were 0.1 mM, 1 mM and 4.0 mM, respectively. ν_{HK}, rate of the hexokinase reaction; ν_{PFK}, rate of the phosphofructokinase reaction; ν_{lower}, rate of the lower part of glycolysis; ν_{ATPase}, rate of the ATPase reaction.

If, however, direct feedback inhibition by hexose monophosphate was used, rather than inhibition through Tre 6-*P* (in such a way that the same steady state would have been reached at the high extracellular glucose concentration), the model performed much worse than the Tre 6-*P* inhibition model: the ATP level and the flux through glycolysis were now less than a tenth of those of the *TPS1* deletant (Table I). This is explained as follows: in order to achieve the same inhibition by Tre 6-*P* or hexose monophosphate at high glucose concentrations, the inhibitory constant of hexose monophosphate needed to be much smaller than that of Tre 6-*P* (see legend to Table I); this stronger inhibition would then be a liability at the low glucose concentration.

Inhibition through an external effector introduces an extra layer of regulation [i.e. regulation of the regulator (Tre 6-*P*) by the hexose monophosphate concentration and possibly other factors], thereby increasing the dynamic range of the inhibition under highly variable environmental conditions. As a consequence, a regulatory mechanism is obtained that limits the turbo effect at high, but not at low, glucose concentrations. This could be the reason why indirect feedback through Tps1p is preferred – as opposed to feedback through direct product inhibition. It should be noted that expression of the *TPS1* gene is glucose repressed[17,24] and the activity of the Tps1p protein is controlled by post-translational modification[25]. The dynamic range of inhibition by Tps1p is therefore not only enlarged by the specific kinetics of the enzyme, but also by controls at the levels of gene expression and protein specific activity.

It is interesting to note that the conditions under which trehalose metabolism is active coincide with the conditions under which the danger of the turbo design of glycolysis is potent: that is, in glucose-derepressed cells where the lower part of glycolysis is not induced. It appears that Tps1p has evolved to play a dual role: trehalose formation under glucose limitation; and feedback regulation on subsequent sudden exposure to glucose excess.

The danger of pathways with turbo design

It is important to note that the problems that we have analysed in this paper are quite specific to pathways that have what we term a 'turbo design'. If, in transitions where substrate becomes suddenly available in excess, there are bottlenecks further down in the pathway, then 'turbo pathways' are especially vulnerable. As its coupling to ATP hydrolysis renders the activating step thermodynamically irreversible, regulation of the rate of that step cannot occur at the level of mass action[26]. Regulation is therefore needed at the level of enzyme activity. Whereas adaptation to a new environment through regulation of gene expression and protein turnover takes place on

Box 2. How can ATP be at steady state whereas the hexose phosphates are not?

Figure 3 shows that feedback inhibition of the hexokinase (HK) module or a reduction in its V_{max} both allowed glycolysis to achieve a steady state. How do we understand this? In **(a)**, the rate characteristics (with respect to ATP) of the four modules in the core model are shown at saturating concentrations of hexose monophosphate (HMP) and fructose 1,6-bisphosphate (Fru 1,6-P_2), because the concentrations of these species are very high in the *tps1-Δ* mutant. HK (K_m for ATP of 0.15 mM) and ATPase (K_m for ATP of 3 mM) show Michaelis–Menten hyperbole (see Box 1). PFK is only very slightly inhibited by ATP at the saturating fructose 6-phosphate concentration, whereas the lower part of glycolysis is indirectly sensitive to ATP. This is because the sum of the ATP and ADP concentrations is set to be constant (5 mM) in the core model (see Box 1). The lower part of glycolysis is taken to follow the rate of PFK – up to the V_{max} of the former (20 mM min^{-1}). From **(a)** it should be concluded that the only 'complete' steady state, where the rates of the HK and PFK reactions and the lower part of glycolysis were equal, would be at an ATP concentration of zero. This is not the state that is reached in the model (unless the initial state was close to this state).

The energetic implications of **(a)** are shown in **(b)**, where the rates of the HK, PFK and ATPase reactions in **(a)** are summed to give the total rate of ATP consumption, and the total rate of ATP production is equal to four times the rate of the lower part of glycolysis (see Eqn 2). The two curves intersect at a point (other than [ATP] = 0) where ATP production equals ATP consumption and, therefore, the concentration of ATP remains constant. This 'ATP-steady' state is stable, because an increase in ATP concentration leads to a higher consumption rate and, consequently, a reduction in ATP concentration. At the 'ATP-steady' state, however, the rates of the HK and PFK reactions, and the lower part of glycolysis are not equal **(a)**; therefore no true steady state is achieved (see Eqn 2). This explains the observed patterns in metabolites: the only way for the lower part of glycolysis to slow down either the PFK or the HK reaction is through the ATP level; however, the ATP level is trapped in an 'ATP-steady' state and accumulation of sugar phosphate can only continue. Changes in the level of ATP cannot cause changes in the reaction rates of HK, PFK, the lower part of glycolysis and the ATPase that would give rise to a 'carbon-steady' state as well.

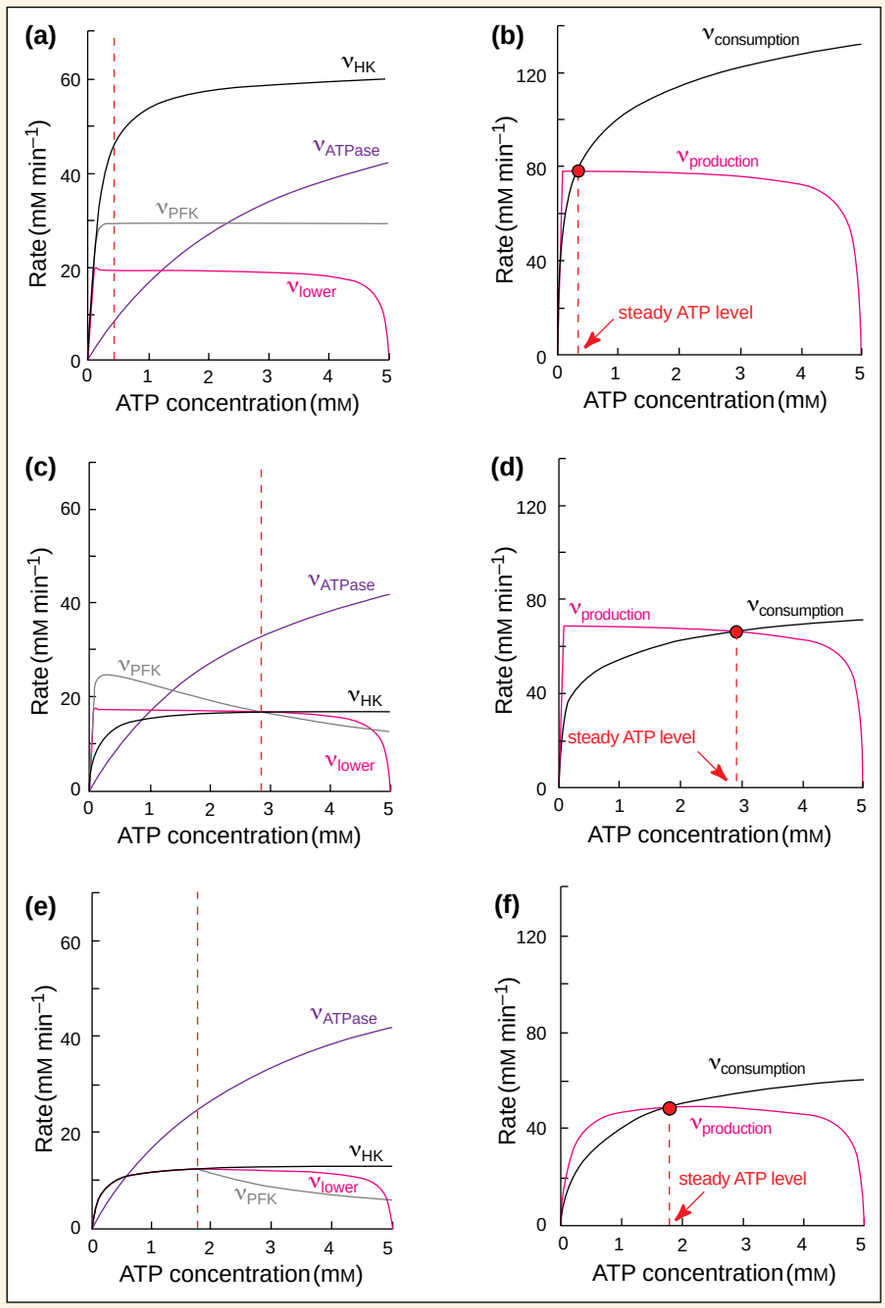

Rate characteristics of the steps of the core model with respect to the ATP concentration. ν_{HK}, rate of the hexokinase reaction; ν_{PFK}, rate of the phosphofructokinase reaction; ν_{lower}, rate of the lower part of glycolysis; ν_{ATPase}, rate of the ATPase reaction; $\nu_{consumption}$, rate of ATP consumption; $\nu_{production}$, rate of ATP production.

(c) and **(d)** show a similar analysis for the wild-type situation (i.e. with feedback inhibition of HK). The ATP dependence of the rates is now analysed at the steady-state levels of HMP and Fru 1,6-P_2 **(c)**. The rate of the lower part of glycolysis again follows the rate of the PFK reaction – up to the V_{max} of the former. A flux-control analysis[45–49] of the steady state shown in Fig. 3c,d broke down as follows: HK, 40 %; PFK, 34%; ATPase, 25% (a flux control of 50% by an enzyme means that an increase of 1% in the activity of that enzyme leads to an increase in the steady-state flux of 0.5%). The lower part of glycolysis exerted no control on the flux, which justifies its dependence on the rate of the PFK reaction. The total flux control is 100%.

As a consequence of the lowered rates of the HK and PFK reactions, there is a steady state for ATP at a higher ATP level **(d)**. Importantly, at this ATP level (and of course at the corresponding HMP and Fru 1,6-P_2 levels), the rates of the HK and PFK reactions, and that of the lower part of glycolysis, are equal, and each is half the rate of the ATPase reaction – phenomena that are compatible with a complete steady state (Eqn 2). Inhibition of PFK by ATP is crucial in this case, because it decreases PFK activity to a level with which the lower part of glycolysis can cope.

(e) and **(f)** show the analysis performed for the case where HK activity is reduced to 22% of the wild-type level. HK completely controls the flux (its flux control amounted to 114% and that of the ATPase amounted to −14%; the flux control coefficients of PFK and the lower part of glycolysis were zero). The rate of the PFK reaction and that of the lower part of glycolysis therefore follow the rate of HK – until the ATP concentration becomes inhibitory (at >1.7 mM). The reduced activity of HK causes the flux through HK to be (just) small enough to allow the lower part of glycolysis to proceed, and a true steady state is reached. In this case, therefore, the need to regulate HK activity is relieved by removing its excess capacity.

Table I. Steady-state concentrations and rates for different versions of the core model of glycolysis, at an extracellular glucose concentration of 0.1 mM, rather than 10 mM.

Model	[HMP] (mM)	[Fru 1,6-P_2] (mM)	ATP (mM)	ν_{HK} (mM min^{-1})	ν_{PFK} (mM min^{-1})	ν_{lower} (mM min^{-1})	ν_{ATPase} (mM min^{-1})
tps1-Δ	2.1	0.3	0.5	4.7	4.7	4.7	9.4
reduced HK	0.8	0	0	0	0	0	0
Tre 6-P inhibition	1.4	0.2	0.3	2.75	2.75	2.75	5.5
HMP inhibition	0.8	0.02	0.04	0.45	0.45	0.45	0.9

The direct feedback inhibition of HK by hexose monophosphate (HMP) is set so as to reach the same steady state as that for Tre 6-*P* inhibition at the high glucose concentration of 10 mM. The K_i of HK for Tre 6-*P* was therefore 11.06 times higher than that for HMP. This is because, rather than $[\text{Tre 6-}P]/K_{i,\text{Tre 6-}P} = [\text{HMP}]^2/K_{i,\text{Tre 6-}P}$, one has the term $[\text{HMP}]/K_{i,\text{HMP}}$ in the nominator of the rate equation for HK (see Box 1), which means that $K_{i,\text{Tre 6-}P} = [\text{HMP}]*K_{i,\text{HMP}}$. The concentration of HMP was 11.06 mM in the steady state in Fig. 3c.

a timescale of minutes to hours, accumulation of intermediates can occur in seconds. We therefore expect that kinetic signals, and not adaptive ones, are required to communicate dangerous metabolic bottlenecks, following a sudden transition to a state of plentiful substrate availability. These fast kinetic signals allow the slower adaptive responses (which could also remove existing bottlenecks) time to take effect. In *S. cerevisiae*, glucose induction of the lower part of glycolysis goes hand in hand with glucose repression of *TPS1* gene expression.

ATP levels might initially be thought of as a good and sufficient kinetic signal (in the short term), because the first step of glycolysis uses ATP as a substrate. A step that is driven by ATP hydrolysis should be considered to be an ATPase and, if it proceeds too fast, the resultant decrease in ATP levels should automatically slow down such a step. No additional regulation would be needed; regulation would merely be a matter of sufficient sensitivity of the first step to ATP. However, increasing the sensitivity of HK for ATP in our core model (by decreasing the affinity of hexokinase for ATP from 0.15 mM to 5 mM) did not prevent the accumulation of hexose phosphate, and the ATP level became constant [at 2.7 mM (B. Teusink, M. C. Walsh, K. van Dam and H. V. Westerhoff, unpublished)].

Our analysis has pointed to the specific danger that pathways with turbo design face: the fact that the steps after the activated one produce a *surplus* of ATP can lead to a state in which ATP consumption and ATP production are equal – even when the flux through the carbon skeleton is not in steady state (see Eqns 1 and 2). Under these conditions, accumulation of intermediates could continue, but the 'trapped' ATP would be unable to signal the failure of the rest of the pathway. This phenomenon has been observed in the *tps1-Δ* mutant of *S. cerevisiae*, but is a potential danger for all activated pathways where the activity of the activated (ATP-consuming) step is in excess of that of the ATP-generating steps. Indeed, substrate-accelerated death of wild-type *S. cerevisiae*, following growth under maltose limitation and subsequent pulsing with excess maltose, has been attributed to an unrestricted uptake of maltose while ATP levels remained relatively constant[6].

In yeast, maltose is actively taken up by a proton symporter[27] and can therefore be considered to be an ATP-consuming step – glycolysis as a whole producing at least four molecules of ATP for each molecule of maltose transported. Furthermore, substrate-accelerated death in bacteria is associated with a repression/derepression mechanism[28,29] – an observation that also points to poor (or too slow) adaptation to a sudden change in the environment. Another good example is 'lactose killing', which occurs when *Escherichia coli* grown in a lactose-limited continuous chemostat are plated on lactose plates: 85–98% of the cells die, because of excessive uptake of lactose[30].

In *Trypanosoma brucei*, compartmentalization of glycolysis into the glycosome overcomes problems caused by the turbo design of glycolysis: inside the glycosome, glycolysis proceeds as far as the generation of 3-phosphoglycerate, which is then transported into the cytosol, where it yields ATP through the pyruvate kinase reaction. There are therefore two pools of ATP, and the part of glycolysis that occurs in the glycosome invests as much (glycosomal) ATP in the HK and PFK steps as it produces in the phosphoglycerate kinase reaction. Indeed, an example of feedback regulation of HK has not been found[31]. A kinetic model of Trypanosome glycolysis[32], in which the compartment boundaries were removed and hence the turbo design of glycolysis restored, showed accumulation of hexose phosphate to extremely high and unrealistic levels (B. M. Bakker, pers. commun.).

The danger of accumulation of intermediates can only effectively be cleared through some feedback inhibition of the ATP-activated step by a means other than the ATP concentration. Direct product inhibition might work for cells in organisms with extracellular homeostatic mechanisms or constant substrate supply, but probably does not have the dynamic range required by cells that live (or have evolved) under highly variable environmental conditions (see Table I). Substrate-accelerated death could therefore be related to the absence of specific regulatory mechanisms that prevent activated pathways with a turbo design demanding their toll before proper adaptation to the new environment has occurred. The ubiquity of activated pathways suggests that there are a number of genes that will produce apparently paradoxical phenotypes when deleted: that is, growth defects, at improved metabolic rates, that arise because of (sudden) substrate availability.

Acknowledgements

We thank Jannie Hofmeyr, Johan Thevelein, Jacky Snoep, Mike Schepper and Barbara Bakker for discussions, suggestions, and critical reading of the manuscript. We also acknowledge the financial assistance of the Foundation for Chemical Research (SON), which is subsidized by the Netherlands Organization for Scientific Research (NWO), the Netherlands Association of Biotechnological Research Centres (ABON) and the European Union through a grant to M. C. W. (grant number BIO4 CT950107 of the BIOTECH programme).

References

1 Bernard, S. A. (1988) *Cell. Biophys.* 12, 119–132
2 Heinrich, R. *et al.* (1997) *Eur. J. Biochem.* 243, 191–201
3 Melendez-Hevia, E., Waddell, T. G., Heinrich, R. and Montero, F. (1997) *Eur. J. Biochem.* 244, 527–543
4 Postgate, J. R. and Hunter, J. R. (1963) *Nature* 198, 273
5 Calcott, P. H. and Postgate, J. R. (1972) *J. Gen. Microbiol.* 70, 115–122
6 Postma, E. *et al.* (1990) *Yeast* 6, 149–158
7 Rizzi, M. *et al.* (1996) *Biotechnol. Bioeng.* 49, 316–327
8 Van der Poll, K. W., Kerkenaar, A. and Schamhart, D. H. (1974) *J. Bacteriol.* 117, 965–970
9 Navon, G. *et al.* (1979) *Biochemistry* 18, 4487–4498
10 Breitenbach-Schmitt, I., Schmitt, H. D., Heinisch, J. and Zimmermann, F. K. (1984) *Mol. Gen. Genet.* 195, 536–540
11 Hohmann, S. *et al.* (1992) *J. Bacteriol.* 174, 4183–4188

12 Van Aelst, L. *et al.* (1993) *Mol. Microbiol.* 8, 927–943
13 Thevelein, J. M. and Hohmann, S. (1995) *Trends Biochem. Sci.* 20, 3–10
14 Bell, W. *et al.* (1992) *Eur. J. Biochem.* 209, 951–959
15 Vuorio, O. E., Kalkkinen, N. and Londesborough, J. (1993) *Eur. J. Biochem.* 216, 849–861
16 Panek, A. D. and Panek, A. C. (1990) *J. Biotechnol.* 14, 229–238
17 Francois, J., Neves, M-J. and Hers, H-G. (1991) *Yeast* 7, 575–587
18 Van Aelst, L. *et al.* (1991) *EMBO J.* 10, 2095–2104
19 Hohmann, S. *et al.* (1993) *Curr. Genet.* 23, 281–289
20 Hohmann, S. *et al.* (1996) *Mol. Microbiol.* 20, 981–991
21 Luyten, K. *et al.* (1993) *Eur. J. Biochem.* 217, 701–713
22 Blazquez, M. A., Lagunas, R., Gancedo, C. and Gancedo, J. M. (1993) *FEBS Lett.* 329, 51–54
23 Thevelein, J. M. (1992) *Antonie van Leeuwenhoek Int. J. Gen. Mol. Microbiol.* 62, 109–130
24 Winderickx, J. *et al.* (1997) *Mol. Gen. Genet.* 252, 470–482
25 Panek, A. C., de Araujo, P. S., Moura Neto, V. and Panek, A. D. (1987) *Curr. Genet.* 11, 459–465
26 Hofmeyr, J-H. S. (1995) *J. Bioenerg. Biomembr.* 27, 479–490
27 Serrano, R. (1977) *Eur. J. Biochem.* 80, 97–102
28 Calgott, P. H. and Postgate, J. R. (1972) *J. Gen. Microbiol.* 70, 115–122
29 Calgott, P. H. and Calvert, T. J. (1981) *J. Gen. Microbiol.* 122, 313–321
30 Dykhuizen, D. and Hartl, D. (1978) *J. Bacteriol.* 135, 876–882
31 Bakker, B. M., Westerhoff, H. V. and Michels, P. A. M. (1995) *J. Bioenerg. Biomembr.* 27, 513–525
32 Bakker, B. M., Michels, P. A. M., Opperdoes, F. R. and Westerhoff, H. V. (1997) *J. Biol. Chem.* 272, 3207–3215
33 Schuster, S., Kahn, D. and Westerhoff, H. V. (1993) *Biophys. Chem.* 48, 1–17
34 Teusink, B. *et al.* (1996) in *BioThermoKinetics of the Living Cell* (Westerhoff, H. V. *et al.*, eds), pp. 417–421, BioThermoKinetics Press, Amsterdam
35 Teusink, B. *et al.* (1998) *J. Bacteriol.* 180, 556–562
36 Viola, R. E., Raushel, F. M., Rendina, A. R. and Cleland, W. W. (1982) *Biochemistry* 21, 1295–1302
37 Londesborough, J. and Vuorio, O. E. (1993) *Eur. J. Biochem.* 216, 841–848
38 Monod, J., Wyman, J. and Changeux, J-P. (1965) *J. Mol. Biol.* 12, 88–118
39 Hess, B. and Plesser, T. (1978) *Ann. New York Acad. Sci.* 316, 203–213
40 Galazzo, J. L. and Bailey, J. E. (1990) *Enzyme Microbiol. Technol.* 12, 162–172
41 Chambers, A., Packham, E. A. and Graham, I. R. (1995) *Curr. Genet.* 29, 1–9
42 Schmitt, H. D. and Zimmermann, F. K. (1982) *J. Bacteriol.* 151, 1146–1152
43 Buttgereit, F. and Brand, M. D. (1995) *Biochem. J.* 312, 163–167
44 Sauro, H. M. and Fell, D. A. (1991) *Math. Comp. Modelling* 15, 15–28
45 Kacser, H. and Burns, J. A. (1973) *Symp. Soc. Exp. Biol.* 27, 65–104
46 Kacser, H., Burns, J. A. and Fell, D. A. (1995) *Biochem. Soc. Trans.* 23, 341–366
47 Heinrich, R. and Rapoport, T. (1974) *Eur. J. Biochem.* 42, 89–95
48 Westerhoff, H. V. and Van Dam, K. (1987) *Thermodynamics and Control of Biological Free-energy Transduction*, Elsevier, Amsterdam
49 Fell, D. A. (1997) *Understanding the Control of Metabolism*, Portland Press, London

A ferredoxin-like domain in RNA polymerase 30/40-kDa subunits

The 30/40-kDa subunits of DNA-dependent RNA polymerases (EC 2.7.7.6) form a protein family named RPB3/RPC5, with members in animals[1], plants[2], yeasts[3], protozoa[4] and archaea[5,6]. These subunits are essential components of the transcription apparatus in eukaryotes[7] and are also remotely similar to the RpoA bacterial DNA-dependent RNA polymerases (α chain)[6]. The RPB3 subfamily members are subunits of RNA polymerase II (Ref. 7), while the RPC5 subfamily members are subunits of RNA polymerases I and III (Ref. 3). With the complete sequencing of the *Methanococcus jannaschii* genome[8], the RpoD protein (ORF MJ0192) has been found to be highly similar to the RpoD protein from *Sulfolobus acidocaldarius*[9,10], a member of this family. However, while the *M. jannaschii* protein identifies all members of the family with BLAST[11] scores of more than 132 and p-values less than 1.4e-11 in the non-redundant protein database, the *S. acidocaldarius* protein[6] (herein called aRpoD – to distinguish it from the RpoD sigma subunit) in addition identifies ferredoxin domains with scores as high as 120 and p-values as low as 1.2e-09, which have not been recognized before[6].

To further investigate the possibility of an insertion and clarify the intra-family relationships of the 30/40-kDa RNA polymerase subunits, we have obtained the nineteen members known to date*, after eliminating redundancy. These proteins are about 300 residues long, while the resulting multiple alignment[12] extends to 534 residues, with large insertions. Three conserved boxes (herein called A, B and C) clearly correspond to the family signatures (Fig. 1a). The Gibbs sampling technique using Blockmaker[13] defines these blocks at positions 106–149 for box A, 246–288 for box B and 367–396 for box C, in the family alignment. These areas are the most-conserved parts of the family, while the 80-residue region between boxes B and C contains a ferredoxin-like domain

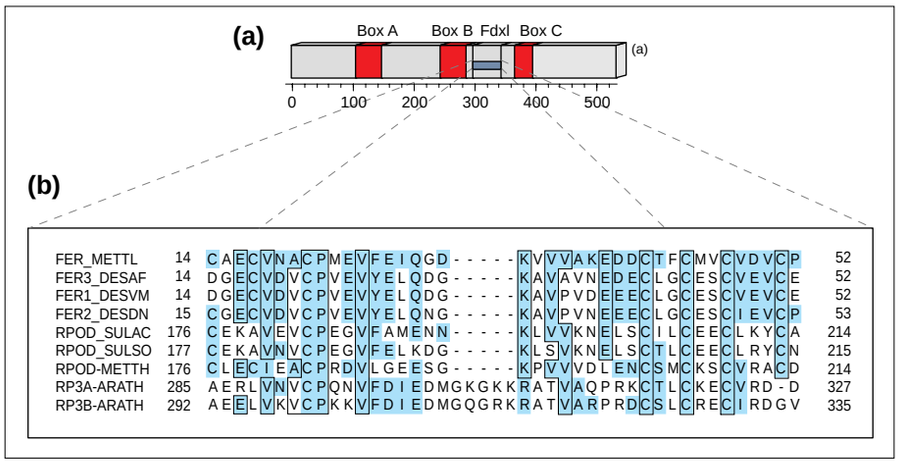

Figure 1

(a) The domain structure of the nineteen known members* of the RPB3/RPC5/aRpoD family. Boxes A, B and C correspond to the most-conserved regions. The total alignment length is 534 residues (see URL: http://www.ebi.ac.uk/~ouzounis/etc/fdxl.html). FdxI is the ferredoxin-like domain present in five members. **(b)** Alignment of the *fdxl* domains from the five RPB3/RPC5/aRpoD members that contain it, with representative members of the ferredoxin family. For naming conventions and accession numbers see Fig. 2. Numbers signify start and end of the domain within the corresponding protein sequences. Invariant residues are boxed and coloring represents hydrophobicity over a window of seven residues.

*Note: after this work was completed, RPOD_METTH (2621073) appeared as ORF_MTH37 (aRpoD) in the complete genome sequence of *Methanobacterium thermoautotrophicum*[19]. In addition, ORF AF2282 from *Archaeoglobus fulgidus*[20] also contains the *fdxl* domain (not shown).

 0968–0004/98/$19.00 PII: S0968-0004(98)01203-1